Fermi National Accelerator Laboratory

FERMILAB-PUB-90/266-T

December 1990

NEUTRINO MASSES AND MIXINGS BASED ON A SPECIAL SET OF QUARK MASS MATRICES

Carl H. ALBRIGHT

Department of Physics, Northern Illinois University, DeKalb, Illinois 60115*

and

Fermi National Accelerator Laboratory, P.O. Box 500, Batavia, Illinois 60510†

Abstract

A special set of quark mass matrices favored by the hadronic flavor-changing data and yielding a top quark mass near 135 GeV is used as input for the leptonic Dirac mass submatrices. A lower bound of $\sin^2 2\theta_{12} = 0.0193$ emerges, which implies a signal less than 25 SNU in the nonadiabatic MSW region for the solar neutrino gallium experiments. By varying the heavy Majorana mass input, we obtain allowed regions in the Δm^2_{23} vs. $\sin^2 2\theta_{23}$ plot which favor a tau neutrino mass in the range 12-120 eV in a very narrow mixing-angle band at 0.0037 or 0.15-5 eV for the $0.004 \lesssim \sin^2 2\theta_{23} \lesssim 0.13$ range.

PACS numbers: 12.15.Ff, 96.40.Tv

*Permanent address

†BITNET Address: ALBRIGHT@FNAL

Operated by Universities Research Association Inc. under contract with the United States Department of Energy

In a series of papers,[1] the author has pursued the subject of quark mass matrices in an effort to find a set which can simultaneously fit all the known data on flavor-changing processes. The data include information on the Cabibbo-Kobayashi-Maskawa[2] (CKM) mixing matrix elements, the ratio $|V_{ub}/V_{cb}|$ entering charmless decays of B mesons, the J-value associated with CP-violation which is proportional to the area of one of the unitarity mixing triangles, $B_d^o - \bar{B}_d^o$ mixing, the K meson bag parameter B_K which enters the theoretical expression for the indirect CP-violation parameter ϵ_K, and the direct-to-indirect CP-violation parameter ratio, ϵ'/ϵ. To achieve a good fit to all this data, it was found necessary to consider a more general set of quark mass matrices than that proposed by Fritzsch,[3] but one can still maintain the spirit of hierarchical chiral symmetry breaking, to wit:

$$\mathbf{M}_U = \begin{pmatrix} 0 & A & D \\ A & E & B \\ D^* & B & C \end{pmatrix}, \qquad \mathbf{M}_D = \begin{pmatrix} 0 & A' & D' \\ A'^* & E & B' \\ D'^* & B'^* & C' \end{pmatrix} \tag{1a}$$

with the relaxed hierarchies

$$\begin{aligned} 0 \lesssim |A|,\ |D|,\ |E| &\ll |B| \ll C \\ 0 \lesssim |A'|,\ |D'|,\ |E'| &\ll |B'| \ll C' \end{aligned} \tag{1b}$$

The top quark mass spectrum obtained through a search of the parameter space exhibits two peaks with the prominent one centered at 135 GeV, in good agreement with the top quark mass predicted by several authors[4] on the basis of neutral-current radiative corrections. Moreover, one very special set of matrices was found[1] which fits all the data remarkably well with only 6 real parameters

$$\mathbf{M}_U = \begin{pmatrix} 0 & A & A \\ A & A & B \\ A & B & C \end{pmatrix}, \qquad \mathbf{M}_D = \begin{pmatrix} 0 & iA' & -A' \\ -iA' & -A' & B' \\ -A' & B' & C' \end{pmatrix} \tag{2}$$

but only in the peak region from 130 - 135 GeV. In contrast, the Fritzsch matrices fail to fit all the data and, at best,[5] yield a top quark mass $\lesssim$ 100 GeV.

In this paper, we extend our analysis to the lepton mass matrices as suggested by grand unified models[6] based on $SO(10)$, flipped $SU(5) \times U(1)$, and $SU(15)$, for example. In doing so, we shall adopt the quark mass matrix forms in (2) above for the lepton Dirac submatrices; the Majorana submatrices are specified below. We generalize Jarlskog's projection operator technique[7] to this situation in order to compute the squares of the mixing matrix elements with high accuracy.

The appearance of Majorana contributions to the neutrino mass matrix requires that we deal with 6×6 matrices. It suffices[8] to set the lefthanded Majorana neutrino entries equal to zero, since the standard model has no Higgs triplets, while the righthanded Majorana neutrino terms can arise from couplings to Higgs singlets or from bare mass terms in the fundamental Lagrangian; for simplicity we choose the submatrix to be diagonal. Thus in the bases $\bar{B}_L = \{\bar{\nu}_{iL},\ (\bar{\nu^c}_i)_L\},\ B_R = \{(\nu_i^c)_R,\ \nu_{iR}\}$ and likewise for the charged leptons, the mass matrices have the following forms

$$M_N = \begin{pmatrix} 0 & \mathbf{M}_N \\ \mathbf{M}_N^T & \mathbf{D}_M \end{pmatrix}, \qquad M_L = \begin{pmatrix} 0 & \mathbf{M}_L \\ \mathbf{M}_L^T & 0 \end{pmatrix} \tag{3}$$

for neutrinos and charged leptons, respectively. We shall identify the forms of the Dirac submatrices according to

$$\mathbf{M}_N = \mathbf{M}_U, \qquad \mathbf{M}_L = \mathbf{M}_D \tag{4a}$$

and take the righthanded Majorana matrix diagonal and equal to

$$\mathbf{D}_M = diag(D_1,\ D_2,\ D_3) \tag{4b}$$

The matrices in the weak basis in (3) are related to the diagonal forms in the mass basis by

$$M_M = U_L^\dagger D_N U_R, \qquad \mathbf{M}_L = U_L'^\dagger \mathbf{D}_L U_R' \tag{5a}$$

in terms of the four unitary transformation matrices $U_L,\ U_R,\ U_L'$ and U_R', and the diagonal mass matrices

$$D_N = diag(\lambda_1,\ \lambda_2,\ \lambda_3,\ \lambda_4,\ \lambda_5,\ \lambda_6), \qquad \mathbf{D}_L = diag(\lambda'_1,\ \lambda'_2,\ \lambda'_3) \tag{5b}$$

where the λ_α and λ'_j are the neutrino and charged lepton masses up to a sign.

The charged-current interactions involve just the lefthanded neutrinos and charged leptons in the weak basis, so in terms of the mass eigenbasis, the counterpart of the quark CKM mixing matrix is 6×3:

$$(V_{CKM})_{\alpha j} = (U_L)_{\alpha i}(U_L^{\prime\dagger})_{ij}, \qquad \alpha = 1-6; \quad i,j = 1,2,3 \tag{6}$$

In order to calculate the squares of the mixing matrix elements, we generalize the projection operator technique of Jarlskog[7] and find

$$|(V_{CKM})_{\alpha j}|^2 = \mathrm{Tr}\left[P_\alpha P'_j\right] = (P_\alpha)_{kl}(P'_j)_{lk} \tag{7a}$$

where

$$\begin{aligned} (P_\alpha)_{kl} &= (U_L^\dagger)_{k\beta}(P^D)_{\beta\beta}(U_L)_{\beta l}, \\ P_\alpha &= \prod_{\gamma\neq\alpha}(\lambda_\gamma \mathbf{I} - M_N)/\prod_{\delta\neq\alpha}(\lambda_\delta - \lambda_\alpha) \qquad (7b) \\ P'_j = U_L^{\prime\dagger} P^{\prime D} U'_L &= \prod_{k\neq j}(\lambda'_k \mathbf{I} - \mathbf{M}_L)/\prod_{l\neq j}(\lambda'_l - \lambda'_j) \qquad (7c) \end{aligned}$$

and P^D and P'^D are the diagonal projection operators. In writing these expressions, we have explicitly made use of the fact that our matrices M_N and $\mathbf{M}_L$ are Hermitian, so that we can take $U_R = U_L$ and $\mathbf{U}'_R = \mathbf{U}'_L$ to diagonalize the matrices. The trace expressions are calculated analytically through use of MACSYMA and then evaluated numerically in a FORTRAN program. To achieve sufficient accuracy (1 part in 10^5), we have used quadruple precision on a VAX computer to calculate the mass eigenvalues λ_α and λ'_j from the characteristic equations.

We begin our search by determining the charged lepton parameters uniquely to be

$$A'_L = 0.007576, \qquad B'_L = 0.4181, \qquad C'_L = 1.686\text{GeV} \tag{8a}$$

from the known charged lepton masses and the invariant properties of the traces and determinant relative to the weak and mass eigenbases. For the special set of quark mass matrices in (2) above with $m_t = 133$ GeV for the best fit to the flavor-changing data, the 6 parameters in $\mathbf{M}_U$ and $\mathbf{M}_D$ are determined at 1 GeV to be

$$\begin{aligned} A_U &= 0.0755, \qquad & B_U &= 17.54, \qquad & C_U &= 213.6 \text{ GeV} \\ A'_D &= 0.0274, \qquad & B'_D &= 0.6782, \qquad & C'_D &= 5.214 \text{ GeV} \end{aligned} \tag{8b}$$

If we neglect the small running effect of the Yukawa couplings, the charged lepton and down quark parameters are scaled by

$$A'_D/A'_L = 3.62, \qquad B'_D/B'_L = 1.62, \qquad C'_D/C'_L = 3.09 \tag{8c}$$

As a starting point, we then note that the neutrino parameters scaled in the same fashion are given by

$$A_N = 0.0209, \qquad B_N = 10.83, \qquad C_N = 69.13 \tag{8d}$$

The diagonal Majorana entries in $\mathbf{D}_M$ remain completely undetermined; however, the well-known seesaw effect[9] for the neutrino mass matrix M_N implies that if all entries in $\mathbf{M}_N$ are increased by a factor of 10 and the diagonal entries in $\mathbf{D}_M$ are increased by a factor of 100, the light neutrino masses remain unchanged. Moreover, the mixing matrix elements $V_{\alpha j}$ are unchanged. Thus in our search of solutions for the masses and mixing angles, we have the freedom to fix $C_N = 69.13$ as in (8d) above and to vary only A_N, B_N and all three D_i.

Our first important observation is that the mixing element $V_{12} \equiv V_{e\mu}$ is totally insensitive to the choice of the D_i's over an extremely large range. Contours in the A_N vs. B_N plane thus correspond to fixed V_{12}. In fact, we find a *minimum* value of V_{12} such that

$$\sin^2 2\theta_{12} \sim 4V_{12}^2 \geq 0.0193 \tag{9}$$

In Fig. 1 we have plotted Δm^2_{12} vs. $\sin^2 2\theta_{12}/\cos 2\theta_{12}$ in the Mikheyev, Smirnov and Wolfenstein[10] (MSW) region, superimposed the solar neutrino capture rate contours[11] or "isoSNU's" for gallium, and imposed the constraint in (9). The interesting conclusion is that the maximum capture rate in the *nonadiabatic* MSW region is expected to be smaller than 25 SNU. The preliminary data from the SAGE experiment[12] are quite consistent with this observation.

Let us now fix $V^2_{12} \simeq \sin^2\theta_{12} = 0.00485$ and adjust $\Delta m^2_{12} \equiv m^2_{\nu_2} - m^2_{\nu_1}$ so that the point lies in the narrow allowed nonadiabatic MSW band corresponding to[13]

$$\Delta m^2_{12}\sin^2\theta_{12} = 1.0 \times 10^{-8}\ \mathrm{eV}^2 \tag{10}$$

i.e., $\Delta m^2_{12} \simeq 2.06 \times 10^{-6}$ eV^2. If we do this by taking all D_i comparable while moving along the fixed $V^2_{12} = 0.00485$ contour in the A_N vs. B_N plane, we traverse the solid curve in the Δm^2_{23} vs. $\sin^2 2\theta_{23}$ plane in Fig. 2a. On the other hand, the point ($V^2_{12} = 0.05$, $\Delta m^2_{12} = 2.0 \times 10^{-7}$ eV^2) in the nonadiabatic MSW region corresponds to the dashed curve in Fig. 2a. Actually, only the points to the right of the short vertical dotted line at $\sin^2 2\theta_{23} = 0.0055$ satisfy the hierarchy condition $B_N/C_N < 0.20$. Thus the region of interest in Fig. 2a is essentially bounded by the solid, dashed and dotted curves, where the closely-spaced dotted curves represent bounds on the excluded region from the E531 experiment[14] at Fermilab and CDHSW[15] at CERN. By choosing the parameters A_N, B_N and C_N equal to those in (8d) for which $V^2_{12} = 0.00488$ and again adjusting the comparable heavy neutrino masses D_i's so that the point lies in the nonadiabatic MSW band with $\Delta m^2_{12} = 2.05 \times 10^{-6}$ eV^2, we obtain the point indicated by the cross in Fig. 1, as well as the corresponding point in Fig. 2a.

Alternatively, we can explore the dependence of Δm^2_{23} and $\sin^2 2\theta_{23}$ on the parameters D_i. For this purpose, we set $V^2_{12} = 0.00485$ at its minimum value again with $\Delta m^2_{12} = 2.06 \times 10^{-6}$ eV^2. We then run through the appropriate contour in the A_N vs. B_N plane for the cases

$$\begin{array}{llll} (1) & D_1 = 10^2 D_2 = 10^4 D_3 & \text{(upper dot -- dashed curve)} & \\ (2) & D_1 = 10 D_2 = 10^2 D_3 & \text{(upper dashed curve)} & \\ (3) & D_1 \sim D_2 \sim D_3 & \text{(solid curve)} & (11) \\ (4) & 10^2 D_1 = 10 D_2 = D_3 & \text{(lower dashed curve)} & \\ (5) & 10^4 D_1 = 10^2 D_2 = D_3 & \text{(lower dot -- dashed curve)} & \end{array}$$

where the description for each case pertains to the curves in Fig. 2b. The dotted curve again gives the loci of points interpolating the 5 cases above for which $B_N/C_N = 0.20$, whereas the closely-spaced dotted curves again represent the present experimental bounds from E531 and CDHSW. The regions of interest in Fig. 2b then lie between these two sets of dotted curves. There is a very narrow allowed band lying along $\sin^2 2\theta_{23} = 0.0037$ with tau neutrino masses in the range $12 \lesssim m_{\nu_\tau} \lesssim 120$ eV. The considerably larger allowed region occurs with $0.15 \lesssim m_{\nu_\tau} \lesssim 5$ eV, and $0.004 \lesssim \sin^2 2\theta_{23} \lesssim 0.13$.

We close with the following observations:

1) Although the charged-current CKM mixing matrix for leptons is 6×3, for all practical purposes it is a unitary 3×3 matrix as the small entries coupling the heavy Majorana neutrinos to the charged leptons are at the level of 10^{-8} or smaller.

2) The V_{12} element is basically dependent upon the ratios B_N/C_N and A_N/C_N and is independent of the heavy Majorana entries D_i. We find a lower bound on $\sin^2 2\theta_{12}$ leading to an upper bound on the solar neutrino capture rate in gallium of 25 SNU in the nonadiabatic MSW region. On the other hand, V_{23} does depend on the values of D_1, D_2 and D_3, especially for the situation where $D_1 << D_2 << D_3$. For $D_1 \sim D_2 \sim D_3$ or the inverted hierarchy, the mixing matrix is essentially determined by the 3×3 Dirac submatrices $\mathbf{M}_N$ and $\mathbf{M}_L$.

3) A relatively "large" 30 - 100 eV tau neutrino mass responsible for closing the universe can only exist if the heavy Majorana mass hierarchy is inverted with $D_1 \gtrsim 30 D_2 \gtrsim 1000 D_3$. The probability for a solution in this region is relatively small, however.

4) The $0.15 \lesssim m_{\nu_\tau} \lesssim 5$ eV mass range is much more likely. The median heavy Majorana

mass lies in the range $(1-5)\times 10^{12}$ GeV. The range for m_{ν_μ} in the nonadiabatic MSW region of interest is $(1-14)\times 10^{-4}$ eV, while m_{ν_e} ranges over $10^{-12}-10^{-6}$ eV.

5) It is apparent from Fig. 2 that great effort should be made to extend the excluded experimental region by one order of magnitude with an upgraded version of E531, for the chances of discovery of neutrino oscillations are large. Such is not the case for the Δm^2_{13} vs. $\sin^2 2\theta_{13}$ plot which is not shown.

6) Of course our precise results rely on the simple form of the matrices in (2), but they provide a good representative picture of the situation. We stress that these matrices explain all the hadronic flavor-changing data remarkably well with a top mass in the most probable range of 130 - 135 GeV, in good agreement with the neutral-current radiative corrections. The heretofore-preferred Fritzsch matrices, on the other hand, fail badly even though they have two extra parameters which can be adjusted.

The author benefitted from several useful conversations with Stephen Parke and thanks him for supplying his updated solar neutrino capture rate contours for gallium. The author also acknowledges the kind hospitality of the Fermilab Theoretical Physics Department. This research was supported in part by Grant No. PHY-8907806 from the National Science Foundation. Fermilab is operated by Universities Research Association, Inc. under contract with the United States Department of Energy.

References

[1] C. H. Albright, Phys. Lett. B **246**, 451 (1990); Fermilab preprint FERMILAB-CONF-90/104-T submitted to the XXV International High Energy Physics Conference, Singapore (1990); Fermilab preprint FERMILAB-CONF-90/196-T, to appear in Proceedings of the XXV Int. HEP Conf., Singapore (1990); and references contained therein.

[2] N. Cabibbo, Phys. Rev. Lett. **10**, 531 (1963); M. Kobayashi and T. Maskawa, Prog. Theor. Phys. **49**, 652 (1973).

[3] H. Fritzsch, Phys. Lett. **70B**, 436 (1977); **73B**, 317 (1978); **166B**, 423 (1986).

[4] J. Ellis and G. L. Fogli, Phys. Lett. B **232** (1989) 139; P. Langacker, Phys. Rev. Lett. **63** (1989) 1920; V. Barger, J. L. Hewett and T. G. Rizzo, Phys. Rev. Lett. **65**, 1313 (1990); J. L. Rosner, Phys. Rev. D **42**, 3107 (1990).

[5] C. H. Albright, Phys. Lett. B **227**, 171 (1989).

[6] R. Johnson, S. Ranfone and J. Schechter, Phys. Lett. **179B**, 355 (1986); G. Lazarides and Q. Shafi, ICTP preprint IC-90-153; I. Antoniadis, J. Ellis, J. S. Hagelin and D. V. Nanopoulos, Phys. Lett.B **231**, 65 (1989); P. H. Frampton and B.-H. Lee, Phys. Rev. Lett. **64**, 619 (1990).

[7] C. Jarlskog, Phys. Rev. D **35**, 1685 (1987); D **36**, 2138 (1987); C. Jarlskog and A. Kleppe, Nucl. Phys. B **286**, 245 (1987).

[8] H. Harari and Y. Nir, Nucl. Phys. B **292**, 251 (1987).

[9] M. Gell-Mann, P. Ramond and R. Slansky, in "Supersymmetry," edited by P. Van Nieuwenhuizen and D. Z. Freedman (North Holland, 1979); T. Yanagida, Prog. Theor. Phys. B **315**, 66 (1978).

[10] S. P. Mikheyev and A. Yu Smirnov, Sov. J. Nucl. Phys. **42**, 913 (1986); Sov. Phys. JETP **64**, 4 (1986); Nuovo Cimento **9C**, 17 (1986); L. Wolfenstein, Phys. Rev. D **17**, 2369 (1978); Phys. Rev. D **20**, 2634 (1979).

[11] S. J. Parke and T. P. Walker, Phys. Rev. Lett. **57**, 2322 (1986).

[12] V. N. Gavrin, in Proceedings of the XXV International Conference on High Energy Physics, Singapore (1990).

[13] S. P. Rosen and S. M. Gelb, Phys. Rev. D **34**, 969 (1986); J. N. Bachall and H. A. Bethe, Phys. Rev. Lett. **65**, 2233 (1990).

[14] N. Ushida et al., Phys. Rev. Lett. **57**, 2897 (1986).

[15] F. Dydak et al., Phys. Lett. B **134**, 281 (1984).

Figure Captions

Figure 1: IsoSNU contours calculated by Parke and Walker for the gallium experiments superimposed on the allowed MSW region indicated by the closely-spaced dotted points. The vertical dotted line marks the lower bound on $\sin^2 2\theta_{12}$ found in our model. The cross indicates the point obtained by the parameter set (8d) when constrained to the nonadiabatic MSW region by an appropriate choice of heavy Majorana masses.

Figure 2: Contours in the Δm^2_{23} vs. $\sin^2 2\theta_{23}$ plane for fixed Δm^2_{12} and $\sin^2 2\theta_{12}$ in the nonadiabatic MSW region, with the ratios A_N/C_N and B_N/C_N and the heavy Majorana masses varying along the curves. In (a) the Majorana masses are taken nearly equal and the solid curve refers to $\Delta m^2_{12} = 2.06 \times 10^{-6}$ eV^2 and $\sin^2 2\theta_{12} = 0.0193$, while the dashed curve refers to $\Delta m^2_{12} = 2.0 \times 10^{-7}$ eV^2 and $\sin^2 \theta_{12} = 0.05$. In (b) the Majorana masses are scaled according to the convention given in (11) with the first choice of points in (a). The dotted curves represent lower bounds for a reasonable hierarchy of parameters ($B_N/C_N < 0.2$). The closely-spaced dotted curves represent the upper bounds from the E531 and CDHSW experiments.

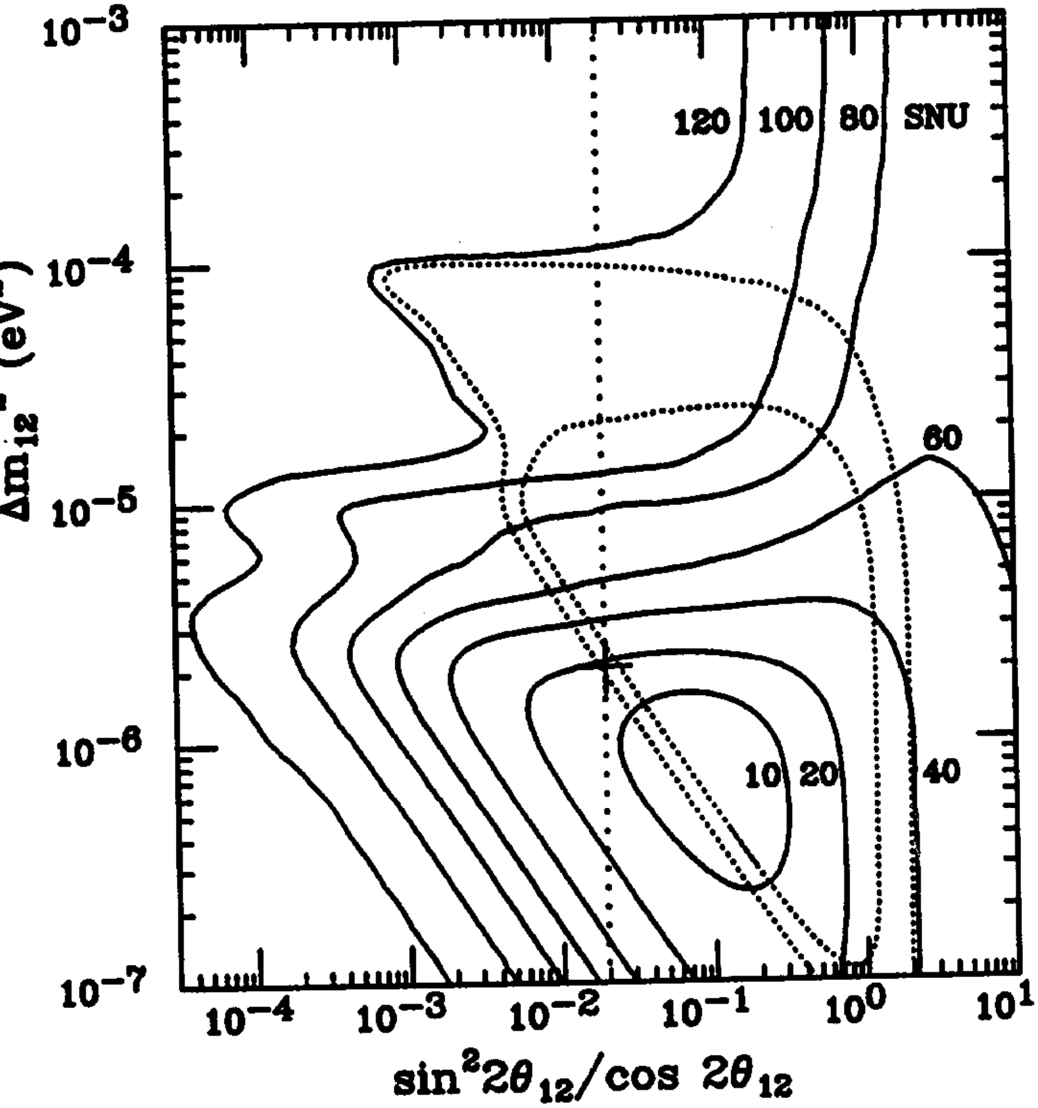

120
100
80
SNU
60
10
20
40
10^{-3}
10^{-4}
10^{-5}
10^{-6}
10^{-7}
Δm_{12}^2 (eV^2)
10^{-4}
10^{-3}
10^{-2}
10^{-1}
10^{0}
10^{1}
$\sin^2 2\theta_{12}/\cos 2\theta_{12}$

Fig. 1

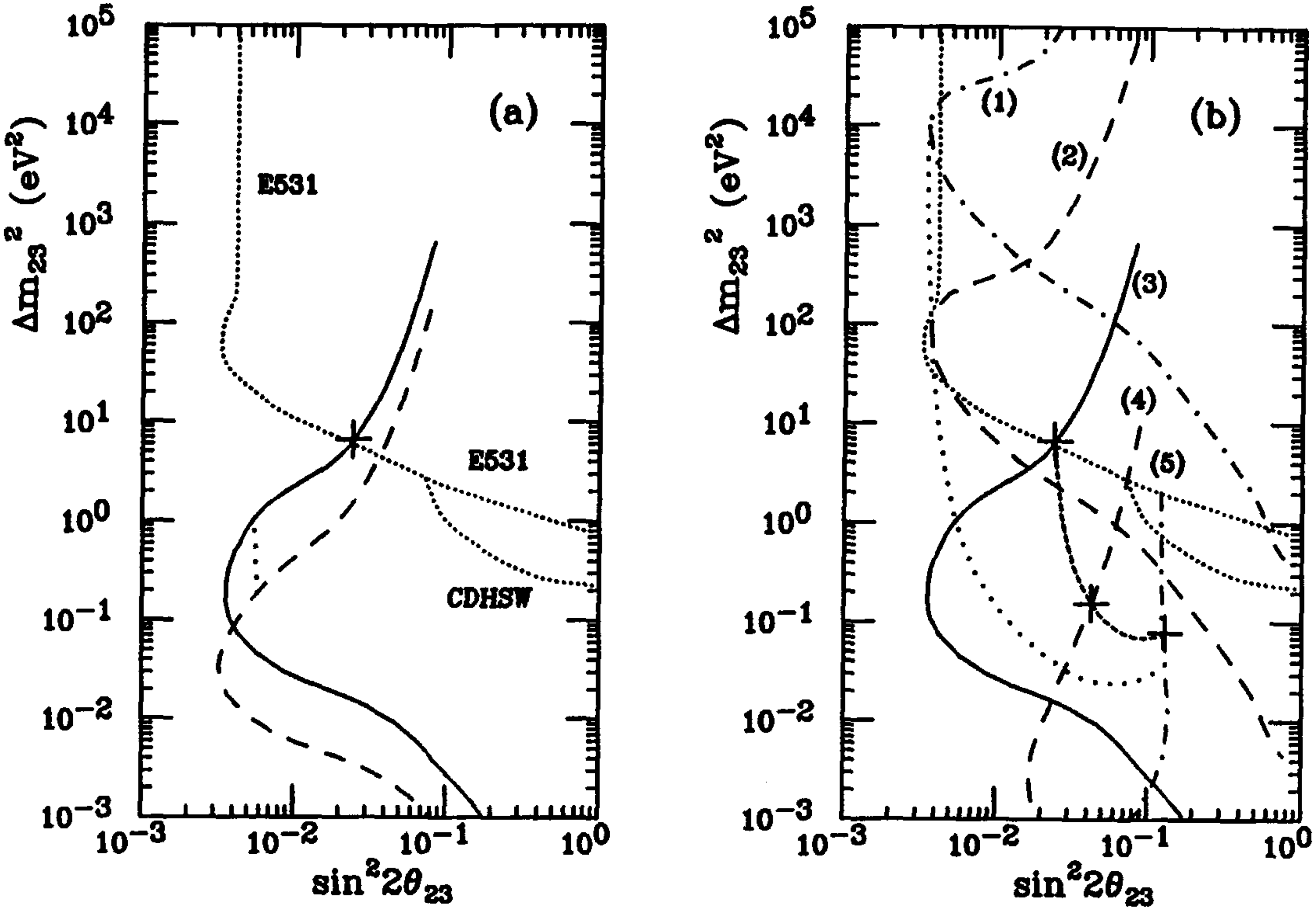
(a)
E531
E531
CDHSW
(b)
(1)
(2)
(3)
(4)
(5)
Δm_{23}^2 (eV^2)
$\sin^2 2\theta_{23}$
10^5
10^4
10^3
10^2
10^1
10^0
10^{-1}
10^{-2}
10^{-3}

Fig. 2